Int J Clin Exp Pathol 2017;10(5):5665-5674
www.ijcep.com /ISSN:1936-2625/IJCEP0049517

Original Article

MicroRNA200c suppresses urothelial carcinoma invasiveness by targeting FSCN1

Mengni Zhang*, Ling Nie*, Zhengzheng Su, Miao Xu, Ni Chen, Jing Gong, Hanbin Xie, Jinjing Zhong, Junya Tan, Yunyi Xu, Xiuyi Pan, Xueqin Chen, Qiao Zhou

*Department of Pathology and State Key Laboratory of Biotherapy, West China Hospital, West China Medical School, Sichuan University, Chengdu, China. *Co-first authors.*

Received January 23, 2017; Accepted February 23, 2017; Epub May 1, 2017; Published May 15, 2017

Abstract: The tumor suppressor miR200c, a metastasis-suppressing miRNA important in epithelial-to-mesenchymal transition (EMT), is down-regulated in many tumor types, including urothelial carcinoma (UC). However, its role in UC cell migration and invasion is still not fully understood. The present study showed miR200c targeted FSCN1, an actin-binding protein important for cell migration. Treatment of UC cells with miR200c mimic simulating artificial overexpression of miR200c reduced FSCN1 level, suppressed UC cell migration and invasion. FSCN1 is a novel post-transcriptional target of miR200c and dysregulation of miR200c-FSCN1 interaction may play a significant role in UC invasion and metastasis.

Keywords: miR200c, FSCN1, urothelial carcinoma

Introduction

Urothelial carcinoma (UC) is the most common malignancy of urinary bladder. Invasive UC comprises about 30% of urinary bladder cancer and is associated with a higher risk of metastasis and poor prognosis [1]. In recent years, invasiveness of UC has been associated with epithelial-to-mesenchymal transition (EMT) and tumor microenvironment. For example, upregulation of TGF-β induces EMT and promotes UC cell invasiveness, which can be suppressed by TGF-β signaling inhibitors [2]. NF-κB, PI3K/Akt and ERK pathways enhance MMP9 expression, which promotes UC cell invasion by degrading the extracellular matrix (ECM) and basement membrane [3-6]. Hypoxia and the transcriptional factor HIF1α have been found to upregulate MMP1 and long non-coding RNA UCA1 in UC, contributing to UC invasiveness [7, 8]. These abnormalities promote of facilitate tumor cell migration, which is an essential component in tumor invasion and is associated with deregulation of cytoskeletons, particularly actin-regulatory molecules, such as fascin1 [9].

The actin-binding protein *Fascin homologue 1* (FSCN1) facilitates cell protrusion by participating in actin bundling, enabling cell migration [10]. Expression of FSCN1 in normal epithelium is low or absent, whereas in tumors such as UC, gastric cancer, non-small cell lung cancer and breast cancer, FSCN1 is up-regulated and promotes tumor cell migration [11-14]. FSCN1 overexpression in cancer may be induced by HIF1α, Sp1 or Smad4 [9, 15, 16], whereas microRNAs, such as miR24, 133a/b, 143, 145, 200b, 326 and 429 may repress FSCN1 expression post transcriptionally [11, 17-21].

MicroRNAs (miRNAs, miRs) post transcriptionally interact with the 3'-UTR of targeted mRNAs and abnormities of miRNAs plays important roles in tumorigenesis and tumor progression [22-24]. The metastasis-repressing miR200c is decreased in various tumors, such as renal cell carcinoma, breast cancer, and gastric cancer [25-27]. Downregulation of miR200c facilitates tumor cell proliferation, metastasis and angiogenesis [23, 28, 29]. Although EMT has been considered to be a major mechanism by which miR200c abnormality may promote tumor inva-

sion, it is not clear whether actin-regulatory molecules such as FSCN1 is also regulated by miR200c, and whether FSCN1's pro-migration function can be inhibited by miR200c.

We observed a close inverse relationship between miR200c and FSCN1 expression in UC samples in preliminary investigations, and hypothesized miR200c might target FSCN1 and suppress tumor cell migration and invasion. Here we report our experimental data demonstrating that FSCN1 is a novel target negatively regulated by miR200c, abnormalities of which contributed to urothelial carcinoma cell migration and invasion.

Materials and methods

Tissues and cell lines

Archived formalin-fixed, paraffin-embedded samples (n=52) and snap-frozen fresh tissue samples (UC tissue, n=3; paired normal urothelial tissue, n=3) were used. All tissue samples were from West China Hospital and were collected and used according to the ethical guidelines and procedures approved by the institutional supervisory committee. All patients were treated with radical cystectomy. Among the patients with archived tissue samples, the age range was from 36 to 80 years (mean, 60.9). The male (n=42, 80.8%) to female (n=10, 19.2%) ratio was 4.2:1. The UCs were graded by the WHO criteria, which included 27 high grade UCs (51.9%) and 25 low grade UCs (48.1%). The tumor-node-metastasis stages of the 52 patients were as follows: stage I (n=4, 7.7%), stage II (n=24, 46.1%), stage III (n=18, 34.7%) and stage IV (n=6, 11.5%).

Human urothelial carcinoma cells RT4 and T24 were from the American Type Culture Collection and were maintained respectively in McCoy's 5A and RPMI 1640 with 10% fetal bovine serum (FBS, Life Technologies, Carlsbad, CA, USA). Tris base, Tween 20, DTT, SDS and EDTA were from Amresco (Solon, OH, USA). Phenylmethylsulfonyl fluoride, leupeptin, pepstatin, and aprotinin were from Roche Diagnostics (Mannheim, Germany).

Stem-loop reverse transcription, reverse transcription-PCR and quantitative real-time PCR

Total RNA was extracted with the Trizol reagent (Invitrogen, Carlsbad, CA, USA). Stem-loop reverse transcription-PCR (RT-PCR) was used to measure mature miR200c level. The stem-loop RT primer for miR200c was designed as 5'-GTC GTA TCC AGT GCA GGG TCC GAG GTA TTC GCA CTG GAT ACG ACT CCA TC-3'. The random RT primer 5'-$(dN)_9$-3' (TaKaRa, Dalian, China) was used for the other genes. The PCR primers for mature miR200c were designed as follows: forward, 5'-GCA TAG CCC GTA ATA CTG CC-3', reverse, 5'-GTG CAG GGT CCG AGG T-3', product length, 67 bp. The PCR primers of FSCN1, GAPDH, U6 were designed according to their respective cDNA sequences (Genbank) as follows: FSCN1 (forward, 5'-CTG CTA CTT TGA CAT CGA GTG G-3', reverse, 5'-GGG CGG TTG ATG AGC TTC A-3', product length, 153 bp), GAPDH (forward, 5'-GGA GCG AGA TCC CTC CAA AAT-3', reverse, 5'-GGC TGT TGT CAT ACT TCT CAT GG-3', product length, 197 bp), U6 (forward, 5'-TGG AAC GAT ACA GAG AAG ATT AGC A-3', reverse, 5'-AAC GCT TCA CGA ATT TGC GT-3', product length, 66 bp). Reverse transcription, conventional PCR, and quantitative real-time quantitative PCR were performed as previously described [22].

Western blot analysis

The primary antibodies used were as follows: FSCN1 (mouse monoclonal, clone number: D-10, 1:1000, Santa Cruz), glyceraldehyde-3-phosphate dehydrogenase (GAPDH; mouse monoclonal, 1:5000, Kangcheng, Shanghai, China). Horseradish peroxidase-labeled secondary antibodies (rabbit monoclonal or mouse monoclonal, 1:5000, Zymed Laboratories, Carlsbad, CA). Western blot analysis was carried out as previously described [22].

miR200c mimic

The miR200c mimic (Ribobio, Guangzhou, China) was used to simulate overexpression of miR200c, and scrambled sequence was used as control.

Immunohistochemistry (IHC) and immunocytochemistry (ICC)

Anti-FSCN1 antibody was used for immunohistochemistry (IHC) and immunocytochemistry (ICC) (mouse monoclonal, clone number: D-10, 1:500, Santa Cruz). Immunostaining was carried out as previously described [30]. Diffuse cytoplasmic staining was interpreted as positive.

Luciferase reporter constructs and site-directed mutagenesis

The seed sequence of FSCN1 3'-UTR (CAGUAUU, 753-759 nt) with flanking sequences was amplified from genomic DNA of HEK293 cells. Target site of FSCN1 3'-UTR was prepared with the primers FSCN1-miR200c-FP (5'-TCT AGA GTT CTG CCA AGG TGG TGG T-3') and FSCN1-miR200c-RP (5'-TCT AGA CAC TCG CTA CTA CAG CCA GG-3'). PCR products were cloned into pMD18-T then subcloned into pGL3-Promoter (Promega, Madison, WI, USA), designated as pGL3-FSCN1-200c-UTR, in which the sequence was inserted into the 3'-UTR downstream of the luciferase coding sequence. Overlapping PCR was used for site-directed mutagenesis of the seed sequences CAGUAUU into GGGGGGG, named pGL3-FSCN1-200c-UTR-MUT. The PCR primers for mutation were as follows: FSCN1-MUT (FP 5'-AAA AAC CCC CCC ATT TGG TC-3', RP 5'-GAC CAA ATG GGG GGG TTT TT-3').

Dual luciferase reporter gene assay

T24 cells were cultured in 24-well plates and transfected with the reporter constructs (0.8 μg) by using Lipofectamine 2000 transfection reagent (Invitrogen, Carlsbad, CA, USA). The pRL-CMV vector (0.02 μg, Promega, Madison, WI) was co-transfected as internal control. Cells were transfected with miR200c mimic or control 24 h after plating and collected 48 h after plating. The renilla and firefly luciferase activities were measured on Luminometer TD-20 (Turner Design, Sunnyvale, CA, USA).

Wound-healing assay

2×10^6 cells were seeded in each well of 6-well plates. A 1 mm scratch across the center of the plate was created with plastic pipette tip after the cells reached confluency. After 24 h culturing in medium with 2% FBS, cell movement into the wound area was examined under microscope. The relative distance between the leading edge was measured using Image-pro plus software (Media Cybernetics) and wound closure was calculated as Wound Closure= $(Width_{0\,h}\text{-}Width_{24\,h})/Width_{0\,h}$.

Transwell cell migration and invasion assays

Both migration and invasion assays were performed (as described [36]) using Transwell inserts (8 μm pore size, Merck Millipore). For migration assays, 1×10^5 cells were seeded in upper chambers with 200 μl RPMI-1640 containing 2% FBS. For invasion assays, 6×10^4 cells were seeded into upper chambers coated with Matrigel (BD Biosciences). The lower chamber contained 10% FBS. After 24 h culture, the membranes were fixed with 4% paraformaldehyde. Cells were stained with crystal violet, and examined under microscope. Six fields were imaged and analyzed by using Image-pro plus.

Immunofluorescence microscopy

Cells were transfected with miR200c mimic or control and cultured on cover glasses, fixed with 4% paraformaldehyde for 30 min, followed by three washes with PBS. Cells were permeabilized with 0.1% Triton X-100 in PBS for 10 min and washed three times with PBS. Then cells were blocked with 3% H_2O_2 for 60 min and 1% goat serum in PBS for 60 min. For examination of F-actin, cover glasses were incubated with ActinGreen (FITC-labelled phalloidin, 1:40 dilution, KeyGEN biotech) and DAPI (1:2000 dilution, KeyGEN biotech) in room temperature. Cover glasses were mounted on slides with ProLong Gold anti-fade reagent (Invitrogen). Olympus FV1000 confocal (Olympus) microscopy was used for imaging.

Statistical analysis

Experiments were independently repeated at least three times. The SPSS 10 program SPSS, Inc., Chicago, IL) was used for statistical analysis. Fisher's exact test was used for between-group comparisons.

Results

FSCN1 was significantly overexpressed in urothelial carcinoma

RT-PCR showed high FSCN1 expression levels in UC cell lines (RT4 and T24) and UC tissues (**Figure 1A**, T1, T2 and T3) but very low or no expression in paired normal urothelial tissues (**Figure 1A**, N1, N2 and N3). Expression of FSCN1 was also higher in T24 than in RT4 (**Figure 1A**).

Q-PCR showed that FSCN1 in UC tissue was 64-fold higher than that of paired normal uro-

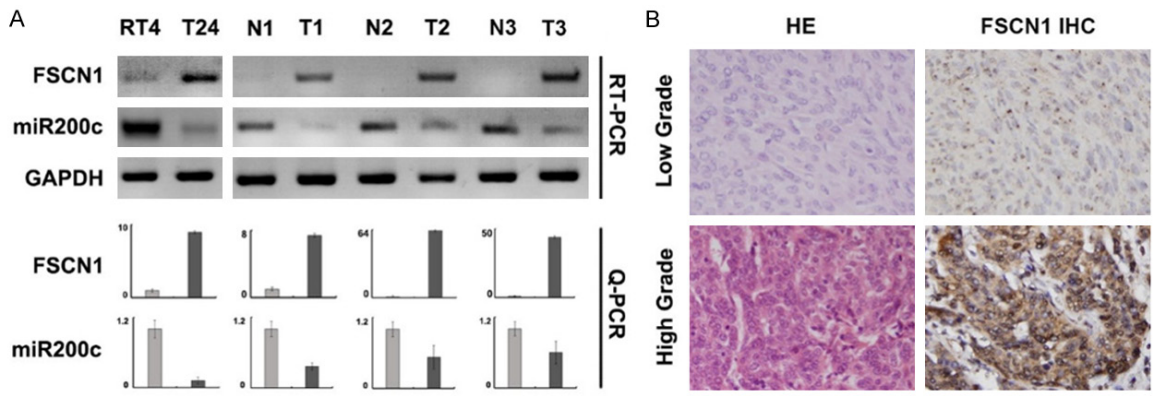

Figure 1. FSCN1 and miR200c expression in UC cell lines (RT4 and T24), UC tissue (T) and paired normal urothelium (N). A. RT-PCR (gel electrophoresis) and Q-PCR (histograms, with GAPDH as internal control) analysis showed FSCN1 expression was higher in UC cell lines and tissue than in paired normal urothelium (P<0.05), and was also higher in high grade UC cell T24 than in low grade RT4 (P<0.05). In contrast, miR200c was significantly lower in UC tissue (T1, T2, T3) than in paired normal urothelium (N1, N2, N3) (P<0.05), and lower in high grade UC cell T24 than in low grade RT4 (P<0.05). B. IHC analysis of FSCN1 expression in formalin-fixed, paraffin-embedded UC samples showed FSCN1 overexpression in high grade UC tissue, but much lower expression or absence in low grade UC samples (P<0.01) (HE: hematoxylin-eosin stained tissue sections; IHC: immunohistochemistry).

thelial tissues. FSCN1 in UC cell lines was 13- to 44-fold higher than that of paired normal urothelial tissues (**Figure 1A**, lower panel, P<0.05).

FSCN1 expression and its relationship with tumor grade and muscle invasion of UC tissue samples (T2 and above) was examined by IHC, which showed significantly higher FSCN1 in high grade UC than in low grade UC (**Figure 1B**). FSCN1 positivity rate was significantly higher in high grade UC samples (25/27, 92.6%) than in low grade UC samples (8/25, 32%, P<0.01). Importantly, FSCN1 positive rate in muscle-invasive UCs (24/31, 77.4%) was significantly higher than in non-muscle-invasive UCs (9/21, 42.9%, P<0.01).

MiR200c was significantly downregulated in urothelial carcinoma

Expression of miR200c was investigated by using stem-loop RT-PCR, which showed high expression levels of miR200c in paired normal urothelial tissues (**Figure 1A**, N1, N2 and N3) but much lower expression levels in UC cell lines (RT4 and T24) and UC tissues (**Figure 1A**, T1, T2 and T3). In addition, expression of miR200c was also significantly lower in the high grade cell line T24 than in the low grade cell line RT4 (**Figure 1A**).

Q-PCR further demonstrated that miR200c in UC tissue and cell lines was significantly decreased in comparison to normal urothelial tissues (**Figure 1A**, low panel, P<0.05). Expression level of miR200c in T24 was even lower than that of RT4 (P<0.05).

FSCN1 was targeted directly by miR200c

TargetScan analysis showed that the 753-759 nt of the FSCN1 3'-UTR was a potential binding site of miR200c, relatively conserved across species (**Figure 2A** and **2B**). Sequence analysis showed no deletion or mutation in the FSCN1 3'-UTR in RT4 and T24 cells (data not shown).

Dual luciferase reporter assay showed that miR200c mimic transfection led to decrease of luciferase reporter gene activity by 39.7± 2.7% in the pGL3-FSCN1 UTR constructs of FSCN1, whereas constructs without FSCN1 3'-UTR sequences were not affected (**Figure 2C**, P<0.05). Mutagenesis of the binding site abolished the inhibitory effect of miR200c on the luciferase gene activity in the pGL3-FSCN1 MUT constructs.

MiR200c mimic led to downregulation of FSCN1

Treatment by miR200c mimic in T24 cells led to significant downregulation of FSCN1 protein expression (**Figure 2D**, western blot, 85.6±2.3%, P<0.05 and **Figure 2E**, ICC, P<0.05). The mRNA level of FSCN1 decreased

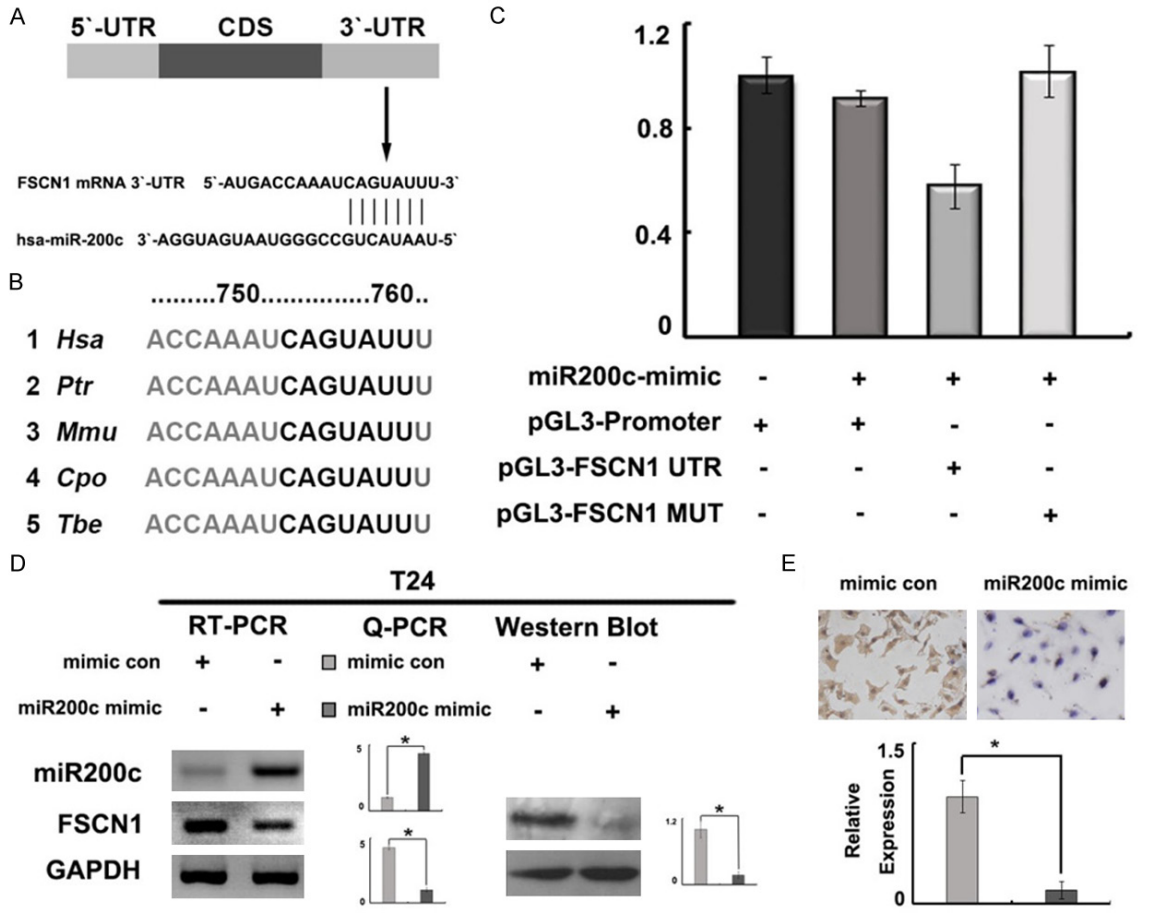

Figure 2. miR200c targeted FSCN1. A. Identification of miR200c seed sequence in FSCN1 3'-UTR. B. Potential seed sequence for miR200c in FSCN1 3'-UTR was conserved across species. C. Dual luciferase reporter gene assays. MiR200c mimic led to decreased (by 39.7±2.7%, $P<0.05$) relative luciferase activity when potential seed sequence was inserted into the downstream of luciferase coding sequence (pGL3-FSCN-UTR), which was restored when the seed sequence was mutated (pGL3-FSCN-MUT). D. RT-PCR and Western blot showed miR200c mimic led to significant decrease of FSCN1 mRNA and protein levels ($P<0.05$). E. Immunocytochemistry showing miR200c mimic treatment resulted in downregulated FSCN1 protein level in cultured cells ($P<0.05$). (UTR: untranslated region; RT-PCR: reverse transcription polymerase chain reaction; con: control; GAPDH: glyceraldehyde-3-phosphate dehydrogenase).

by 76.6±1.9% after miR200c mimic treatment ($P<0.05$).

Overexpression of miR200c repressed cell migration and invasion

The Transwell migration assay showed that the number of migrating cells decreased by 87.5±0.4% with miR200c mimic treatment compared with control (**Figure 3A**, $P<0.05$). Similarly, Transwell invasion assay showed that the number of invading cells decreased by 80.2±1.0% with miR200c mimic transfection (**Figure 3B**, $P<0.05$).

The wound healing assay showed cell mobility and migration was inhibited significantly by miR200c mimic transfection (% of wound closure; blank: 100.0±2.1, control: 100.0±1.8; miR200c: 37.9±2.8; $P<0.05$; **Figure 3C**).

MiR200c mimic effects on actin cytoskeleton

FITC-labelled phalloidin was used to stain F-actin. Immunofluorescence microscopy showed F-actin depolymerization and redistribution with miR200c mimic treatment, indicating suppression of F-actin bundling by miR200c (**Figure 3D**).

Discussion

Ability to invade surrounding tissue and to metastasize is a hallmark of malignancy and

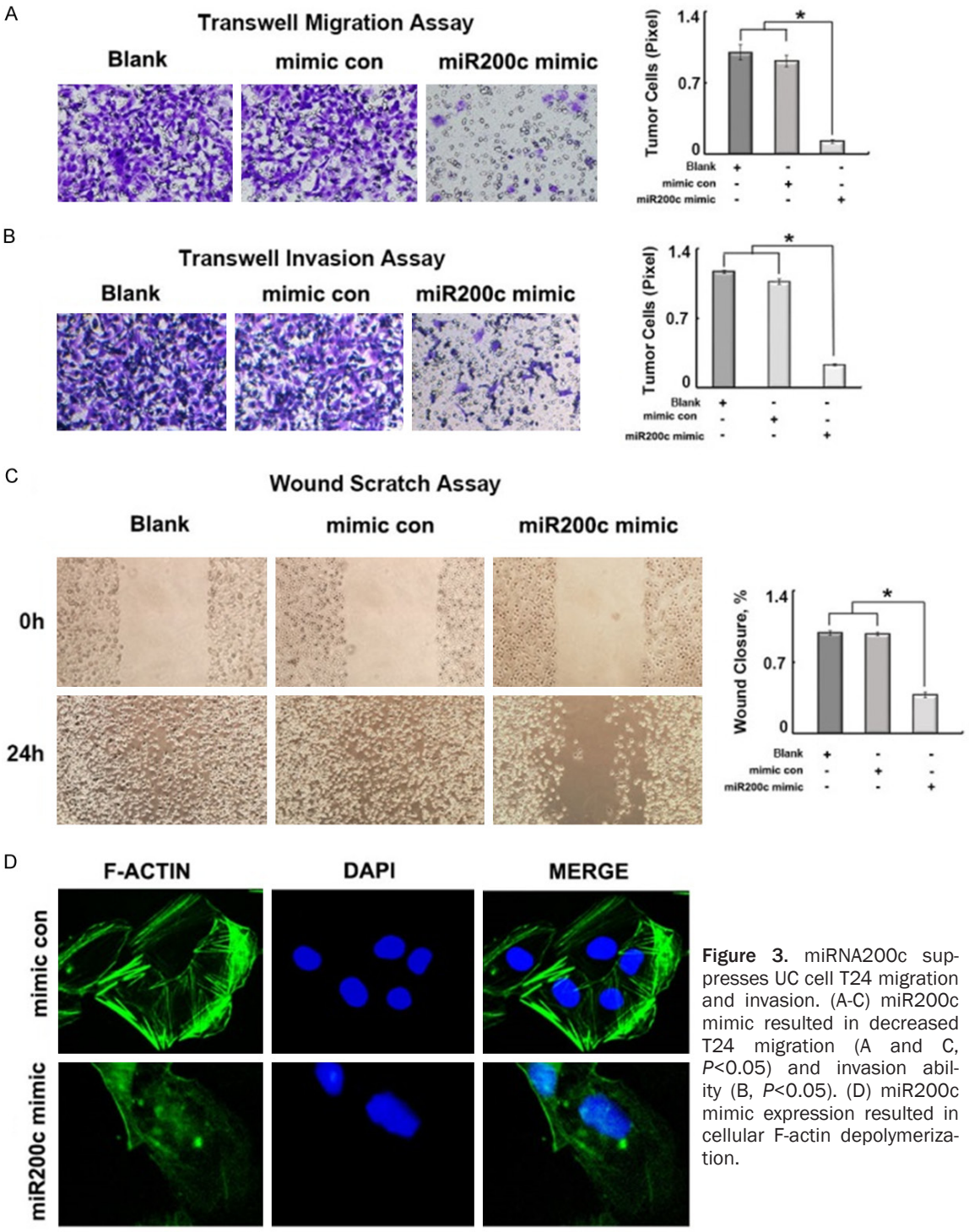

Figure 3. miRNA200c suppresses UC cell T24 migration and invasion. (A-C) miR200c mimic resulted in decreased T24 migration (A and C, $P<0.05$) and invasion ability (B, $P<0.05$). (D) miR200c mimic expression resulted in cellular F-actin depolymerization.

also a leading cause of death for tumor patients [31]. The mechanisms of metastasis are extremely complex and are under intensive investigation. These include the cytoplasmic machineries controlling cell migration (notably actin-regulating molecules involved in the formation of filopodia, lamellipodia and invadopodia), signalling and adhesion molecules determining cell-cell and cell-matrix interactions, and enzymes that are able to degrade extracellular matrix (ECM) (such as matrix metalloproteases, MMPs). Many recent studies focused

on epithelial-mesenchymal transition (EMT) and tumor microenvironment for their roles in tumor invasion and metastasis. For epithelial tumors such as UC, high invasive and metastatic abilityis associated with an acquired mesenchymal phenotype through the process of EMT, which confers the capacity to degrade ECM and to migrate. EMT of carcinoma cells leads to loss of epithelial markers, such as E-cadherin but gain of mesenchymal markers, such as vimentin [32, 33]. The tumor microenvironment can alsobe modified by tumor cells to promote tumor cell proliferation, migration and invasion [34]. For example, hypoxic microenvironment helps to recruit macrophages and induces CCL4-CCR5 and MMP9 expression to degrade ECM and to promote glioblastoma invasion [35].

Many molecules and pathways have been implicated in UC cell migration and invasion, including those involved in EMT and tumor microenvironment. For example, ZEB1, Snail1, Slug and Twist, key regulators in EMT, are upregulated and highly correlated to muscle invasiveness and poor prognosis of UC [36]; whereas E-cadherin expression has an inverse relationship with invasiveness and lymph node metastasis of UC [37]. Hypoxia and HIF1α may directly up-regulate ZEB1 and repress tumor suppressor gene C/EBPα expression [38]. CD4+ T cellsrecruited by UC cells secrete interleukin-1 into tumor microenvironment and activate AR-HIF1α-VEGFa signalling to promote UC cell invasion [39]. UC cells also recruit mast cells and neutrophils to facilitate UC cell migration via ERβ/CCL2/CCR2/EMT/MMP9 signalling [40]. Aberrant transcriptional activation of MMP9 by NF-κB, ERK and PI3K/Akt pathways leads to ECM and basement membrane degradation to promote tumor metastasis [3-5]. Despite the importance of EMT and tumor microenvironment which facilitate tumor cell migration and invasion, the most direct determinants of tumor cell migration are molecules responsible for cell movement, particular those involved in actin regulation, such as cofilin.

Fascin homologue 1 (FSCN1) is a 55 kD actin-binding protein encoded by *FSCN1* gene on chromosome 7p22. The two actin-binding sites, aa33-47 within β-trefoil-1 and aa277-493 within β-trefoil-3 of FSCN1, enable its binding to actin molecules and to facilitate formation and stabilization of filopodia, lamellipodia or invadopodia involve in cell migration [41]. Downregulation of FSCN1 by siRNA reduces the formation of filopodia [42]. FSCN1 dissociation from focal adhesions (FAs) leads to FA disassembly and inhibits cell migration [43].

In normal epithelium, FSCN1 expression is low or even absent, whereas it is often up-regulated in tumors such as pancreatic, gastric, prostatic, nasopharyngeal, colonic, esophageal and non-small-cell lung cancers [9, 17, 19, 20, 44-46]. Overexpression of FSCN1 is often associated with higher stage (such as in serous ovarian carcinoma) [47], low survival rates (for example, in gastric cancer) [17] and also serves as a potential independent marker of metastasis and prognosis (e.g. in non-small-cell lung cancer) [45]. In oral squamous cell carcinoma, FSCN1 upregulation promotes formation of filopodia, lamellipodia and longer microspikes and is correlated with higher tumor stage, lymph node metastasis and shorter survival time [48].

FSCN1 has been shown to be transcriptionally activated by HIF1α, which binds to the hypoxia response element (HRE) within FSCN1 promoter [9]. FSCN1 is also a direct target of Smad4, the interaction with which can be blocked by GATA3 [16]. Transcriptional factors STAT3, Slug, NF-κB and Sp1 contribute to FSCN1 overexpression in tumors [9, 15, 16]. At posttranscriptional level, miR24, miR133a/b, miR143, miR145, miR326 and miR429 function as tumor-suppressing miRs by targeting FSCN1 [11, 17, 19-21]. MiR200b targets FSCN1 and decreases NSCLC cell migration and invasion [18].

MiR200c is one of the most important tumor suppressor microRNAs and also a metastasis-suppressing miRNA. Several important molecules have been identified as targets of miR200c, including ZEB1, VEGF and BMI1 [27, 49, 50]. In the process of EMT, ZEB1 functions as an crucial EMT inducer, by directly repressing expression of cell adhesion and polarity genes, such as E-cadherin, LGL2 and Crumbs3 [51, 52]. ZEB1 also promotes metastasis by repressing miR200c directly [53, 54]. This double-negative feedback loop is an important regulatory mechanism in maintaining balance between epithelial and mesenchymal states of cells.

MiR200c deregulation has been shown in various types of tumor, including cancer of kidney, lung, breast, colon, liver and esophagus [25-27, 55-57]. Downregulation of miR200c is correlated with tumor grade and prognosis in such tumors as gastric cancer and UC [26, 58]. Though miR200c has been reported to be downregulated in UC and was correlated with tumor grade and infiltration of UC [58, 59], the targets most relevant to tumor cell migration or invasion in UC that are suppressed by miR200c are not clear. Our data showed and that dysregulated miR200c expression resulted in FSCN1 overexpression in UC, whereas simulated miR200c expression significantly decreased FSCN1 expression, cell mobility and invisibility of urothelial cells.

In summary, the present study demonstrated that FSCN1 was a novel target of miR200c, which suppressed UC cell migration and invasion. These findings suggest that disruption of miR200c/FSCN1 regulation may contribute significantly to tumor cell migration and invasion and to tumor progression of UC.

Acknowledgements

Supported by grants from the Natural Science Foundation of China (NSFC) (81272848, 81272820, 81302225, 81402110, 81572540, 81572541).

Disclosure of conflict of interest

None.

Address correspondence to: Drs. Xueqin Chen and Qiao Zhou, Department of Pathology, West China Hospital, West China Medical School, Sichuan University, Chengdu 610041, China. Tel: +86-28-8516-4027; Fax: +86-28-8516-4027; E-mail: zhou_qiao@hotmail.com

References

[1] Kaufman DS, Shipley WU, Feldman AS. Bladder cancer. Lancet 2009; 374: 239-249.

[2] Liang Y, Zhu F, Zhang H, Chen D, Zhang X, Gao Q, Li Y. Conditional ablation of TGF-beta signaling inhibits tumor progression and invasion in an induced mouse bladder cancer model. Sci Rep 2016; 6: 29479.

[3] Gao Y, Guan Z, Chen J, Xie H, Yang Z, Fan J, Wang X, Li L. CXCL5/CXCR2 axis promotes bladder cancer cell migration and invasion by activating PI3K/AKT-induced upregulation of MMP2/MMP9. Int J Oncol 2015; 47: 690-700.

[4] Lee SJ, Cho SC, Lee EJ, Kim S, Lee SB, Lim JH, Choi YH, Kim WJ, Moon SK. Interleukin-20 promotes migration of bladder cancer cells through extracellular signal-regulated kinase (ERK)-mediated MMP-9 protein expression leading to nuclear factor (NF-kappaB) activation by inducing the up-regulation of p21 (WAF1) protein expression. J Biol Chem 2013; 288: 5539-52.

[5] Park SL, Won SY, Song JH, Kim WJ, Moon SK. EPO gene expression induces the proliferation, migration and invasion of bladder cancer cells through the p21WAF1 mediated ERK1/2/NF-kappaB/MMP-9 pathway. Oncol Rep 2014; 32: 2207-14.

[6] Bi JB, Zhu Y, Chen XL, Yu M, Zhang YX, Li BX, Sun JW, Shen HL, Kong CZ. The role of fascin in migration and invasion of urothelial carcinoma of the bladder. Urol Int 2013; 91: 227-35.

[7] Shin DH, Dier U, Melendez JA, Hempel N. Regulation of MMP-1 expression in response to hypoxia is dependent on the intracellular redox status of metastatic bladder cancer cells. Biochim Biophys Acta 2015; 1852: 2593-602.

[8] Xue M, Li X, Li Z, Chen W. Urothelial carcinoma associated 1 is a hypoxia-inducible factor-1alpha-targeted long noncoding RNA that enhances hypoxic bladder cancer cell proliferation, migration, and invasion. Tumour Biol 2014; 35: 6901-12.

[9] Zhao X, Gao S, Ren H, Sun W, Zhang H, Sun J, Yang S, Hao J. Hypoxia-inducible factor-1 promotes pancreatic ductal adenocarcinoma invasion and metastasis by activating transcription of the actin-bundling protein fascin. Cancer Res 2014; 74: 2455-64.

[10] Vignjevic D, Kojima S, Aratyn Y, Danciu O, Svitkina T, Borisy GG. Role of fascin in filopodial protrusion. J Cell Biol 2006; 174: 863-75.

[11] Zhang M, Dong BB, Lu M, Zheng MJ, Chen H, Ding JZ, Xu AM, Xu YH. miR-429 functions as a tumor suppressor by targeting FSCN1 in gastric cancer cells. Onco Targets Ther 2016; 9: 1123-33.

[12] Liang Z, Wang Y, Shen Z, Teng X, Li X, Li C, Wu W, Zhou Z, Wang Z. Fascin 1 promoted the growth and migration of non-small cell lung cancer cells by activating YAP/TEAD signaling. Tumour Biol 2016; 37: 10909-15.

[13] Xue M, Pang H, Li X, Li H, Pan J, Chen W. Long non-coding RNA urothelial cancer-associated 1 promotes bladder cancer cell migration and invasion by way of the hsa-miR-145-ZEB1/2-FSCN1 pathway. Cancer Sci 2016; 107: 18-27.

[14] Alshaker H, Wang Q, Kawano Y, Arafat T, Böhler T, Winkler M, Cooper C, Pchejetski D. Everolimus (RAD001) sensitizes prostate can-

cer cells to docetaxel by down-regulation of HIF-1alpha and sphingosine kinase 1. Oncotarget 2016; 7: 80943-80956.
[15] Lu XF, Li EM, Du ZP, Xie JJ, Guo ZY, Gao SY, Liao LD, Shen ZY, Xie D, Xu LY. Specificity protein 1 regulates fascin expression in esophageal squamous cell carcinoma as the result of the epidermal growth factor/extracellular signal-regulated kinase signaling pathway activation. Cell Mol Life Sci 2010; 67: 3313-29.
[16] Sun J, He H, Pillai S, Xiong Y, Challa S, Xu L, Chellappan S, Yang S. GATA3 transcription factor abrogates Smad4 transcription factor-mediated fascin overexpression, invadopodium formation, and breast cancer cell invasion. J Biol Chem 2013; 288: 36971-82.
[17] Li Y, Gao Y, Xu Y, Ma H, Yang M. Down-regulation of miR-326 is associated with poor prognosis and promotes growth and metastasis by targeting FSCN1 in gastric cancer. Growth Factors 2015; 33: 267-74.
[18] Xiao P, Liu W, Zhou H. miR-200b inhibits migration and invasion in non-small cell lung cancer cells via targeting FSCN1. Mol Med Rep 2016; 14: 1835-40.
[19] Kano M, Seki N, Kikkawa N, Fujimura L, Hoshino I, Akutsu Y, Chiyomaru T, Enokida H, Nakagawa M, Matsubara H. miR-145, miR-133a and miR-133b: tumor-suppressive miRNAs target FSCN1 in esophageal squamous cell carcinoma. Int J Cancer 2010; 127: 2804-14.
[20] Li YQ, Lu JH, Bao XM, Wang XF, Wu JH, Hong WQ. MiR-24 functions as a tumor suppressor in nasopharyngeal carcinoma through targeting FSCN1. J Exp Clin Cancer Res 2015; 34: 130.
[21] Liu R, Liao J, Yang M, Sheng J, Yang H, Wang Y, Pan E, Guo W, Pu Y, Kim SJ, Yin L. The cluster of miR-143 and miR-145 affects the risk for esophageal squamous cell carcinoma through co-regulating fascin homolog 1. PLoS One 2012; 7: e33987.
[22] Chen X, Gong J, Zeng H, Chen N, Huang R, Huang Y, Nie L, Xu M, Xia J, Zhao F, Meng W, Zhou Q. MicroRNA145 targets BNIP3 and suppresses prostate cancer progression. Cancer Res 2010; 70: 2728-38.
[23] Li XL, Chen XQ, Zhang MN, Chen N, Nie L, Xu M, Gong J, Shen PF, Su ZZ, Weng X, Tan JY, Zhao T, Zeng H, Zhou Q. SOX9 was involved in TKIs resistance in renal cell carcinoma via Raf/MEK/ERK signaling pathway. Int J Clin Exp Pathol 2015; 8: 3871-81.
[24] Hu MH, Ma CY, Wang XM, Ye CD, Zhang GX, Chen L, Wang JG. MicroRNA-126 inhibits tumor proliferation and angiogenesis of hepatocellular carcinoma by down-regulating EGFL7 expression. Oncotarget 2016; 7: 66922-66934.
[25] Lin J, Liu C, Gao F, Mitchel RE, Zhao L, Yang Y, Lei J, Cai J. miR-200c enhances radiosensitivity of human breast cancer cells. J Cell Biochem 2013; 114: 606-15.
[26] Tang H, Deng M, Tang Y, Xie X, Guo J, Kong Y, Ye F, Su Q, Xie X. miR-200b and miR-200c as prognostic factors and mediators of gastric cancer cell progression. Clin Cancer Res 2013; 19: 5602-5612.
[27] Jeck WR, Sorrentino JA, Wang K, Slevin MK, Burd CE, Liu J, Marzluff WF, Sharpless NE. Circular RNAs are abundant, conserved, and associated with ALU repeats. RNA 2013; 19: 141-57.
[28] Sulaiman SA, Ab Mutalib NS, Jamal R. miR-200c regulation of metastases in ovarian cancer: potential role in epithelial and mesenchymal transition. Front Pharmacol 2016; 7: 271.
[29] Zhou J, Xu D, Xie H, Tang J, Liu R, Li J, Wang S, Chen X, Su J, Zhou X, Xia K, He Q, Chen J, Xiong W, Cao P, Cao K. miR-33a functions as a tumor suppressor in melanoma by targeting HIF-1alpha. Cancer Biol Ther 2015; 16: 846-55.
[30] Chen N, Chen X, Huang R, Zeng H, Gong J, Meng W, Lu Y, Zhao F, Wang L, Zhou Q. BCL-xL Is a Target Gene Regulated by Hypoxia-inducible Factor-1 alpha. J Biol Chem 2009; 284: 10004-10012.
[31] Marx V. Tracking metastasis and tricking cancer. Nature 2013; 494: 133-6.
[32] Nieto MA. Epithelial-mesenchymal transitions in development and disease: old views and new perspectives. Int J Dev Biol 2009; 53: 1541-7.
[33] Thiery JP, Acloque H, Huang RY, Nieto MA. Epithelial-mesenchymal transitions in development and disease. Cell 2009; 139: 871-90.
[34] Hu Y, Yu X, Xu G, Liu S. Metastasis: an early event in cancer progression. J Cancer Res Clin Oncol 2017; 143: 745-757.
[35] Wang Y, Liu T, Yang N, Xu S, Li X, Wang D. Hypoxia and macrophages promote glioblastoma invasion by the CCL4-CCR5 axis. Oncol Rep 2016; 36: 3522-3528.
[36] Schulte J, Weidig M, Balzer P, Richter P, Franz M, Junker K, Gajda M, Friedrich K, Wunderlich H, Östman A, Petersen I, Berndt A. Expression of the E-cadherin repressors Snail, Slug and Zeb1 in urothelial carcinoma of the urinary bladder: relation to stromal fibroblast activation and invasive behaviour of carcinoma cells. Histochem Cell Biol 2012; 138: 847-60.
[37] Byrne RR, Shariat SF, Brown R, Kattan MW, Morton RA JR, Wheeler TM, Lerner SP. E-cadherin immunostaining of bladder transitional cell carcinoma, carcinoma in situ and lymph node metastases with long-term follow-up. J Urol 2001; 165: 1473-9.
[38] Xue M, Li X, Chen W. Hypoxia regulates the expression and localization of CCAAT/enhancer

binding protein alpha by hypoxia inducible factor-1alpha in bladder transitional carcinoma cells. Mol Med Rep 2015; 12: 2121-7.
[39] Tao L, Qiu J, Jiang M, Song W, Yeh S, Yu H, Zang L, Xia S, Chang C. Infiltrating T cells promote bladder cancer progression via increasing IL1-->androgen receptor-->HIF1alpha-->VEGFa signals. Mol Cancer Ther 2016; 15: 1943-51.
[40] Rao Q, Chen Y, Yeh CR, Ding J, Li L, Chang C, Yeh S. Recruited mast cells in the tumor microenvironment enhance bladder cancer metastasis via modulation of ERbeta/CCL2/CCR2 EMT/MMP9 signals. Oncotarget 2016; 7: 7842-55.
[41] Jayo A and Parsons M. Fascin: a key regulator of cytoskeletal dynamics. Int J Biochem Cell Biol 2010; 42: 1614-7.
[42] Li A, Dawson JC, Forero-Vargas M, Spence HJ, Yu X, König I, Anderson K, Machesky LM. The actin-bundling protein fascin stabilizes actin in invadopodia and potentiates protrusive invasion. Curr Biol 2010; 20: 339-45.
[43] Elkhatib N, Neu MB, Zensen C, Schmoller KM, Louvard D, Bausch AR, Betz T, Vignjevic DM. Fascin plays a role in stress fiber organization and focal adhesion disassembly. Curr Biol 2014; 24: 1492-9.
[44] Sui X, Zhu J, Tang H, Wang C, Zhou J, Han W, Wang X, Fang Y, Xu Y, Li D, Chen R, Ma J, Jing Z, Gu X, Pan H, He C. p53 controls colorectal cancer cell invasion by inhibiting the NF-kappaB-mediated activation of Fascin. Oncotarget 2015; 6: 22869-79.
[45] Teng Y, Xu S, Yue W, Ma L, Zhang L, Zhao X, Guo Y, Zhang C, Gu M, Wang Y. Serological investigation of the clinical significance of fascin in non-small-cell lung cancer. Lung Cancer 2013; 82: 346-52.
[46] Fuse M, Nohata N, Kojima S, Sakamoto S, Chiyomaru T, Kawakami K, Enokida H, Nakagawa M, Naya Y, Ichikawa T, Seki N. Restoration of miR-145 expression suppresses cell proliferation, migration and invasion in prostate cancer by targeting FSCN1. Int J Oncol 2011; 38: 1093-101.
[47] Wen YH, Yee H, Goswami S, Shukla PS. Fascin expression in serous tumors of ovary correlates with aggressiveness of malignancy. Int J Gynecol Pathol 2009; 28: 187-92.
[48] Alam H, Bhate AV, Gangadaran P, Sawant SS, Salot S, Sehgal L, Dange PP, Chaukar DA, D'cruz AK, Kannanl S, Gude R, Kane S, Dalal SN, Vaidya MM. Fascin overexpression promotes neoplastic progression in oral squamous cell carcinoma. BMC Cancer 2012; 12: 32.
[49] Shi L, Zhang S, Wu H, Zhang L, Dai X, Hu J, Xue J, Liu T, Liang Y, Wu G. MiR-200c increases the radiosensitivity of non-small-cell lung cancer cell line A549 by targeting VEGF-VEGFR2 pathway. PLoS One 2013; 8: e78344.
[50] Liu S, Tetzlaff MT, Cui R, Xu X. miR-200c inhibits melanoma progression and drug resistance through down-regulation of BMI-1. Am J Pathol 2012; 181: 1823-35.
[51] Spaderna S, Schmalhofer O, Wahlbuhl M, Dimmler A, Bauer K, Sultan A, Hlubek F, Jung A, Strand D, Eger A, Kirchner T, Behrens J, Brabletz T. The transcriptional repressor ZEB1 promotes metastasis and loss of cell polarity in cancer. Cancer Res 2008; 68: 537-44.
[52] Aigner K, Dampier B, Descovich L, Mikula M, Sultan A, Schreiber M, Mikulits W, Brabletz T, Strand D, Obrist P, Sommergruber W, Schweifer N, Wernitznig A, Beug H, Foisner R, Eger A. The transcription factor ZEB1 (deltaEF1) promotes tumour cell dedifferentiation by repressing master regulators of epithelial polarity. Oncogene 2007; 26: 6979-88.
[53] Park SM, Gaur AB, Lengyel E, Peter ME. The miR-200 family determines the epithelial phenotype of cancer cells by targeting the E-cadherin repressors ZEB1 and ZEB2. Genes Dev 2008; 22: 894-907.
[54] Burk U, Schubert J, Wellner U, Schmalhofer O, Vincan E, Spaderna S, Brabletz T. A reciprocal repression between ZEB1 and members of the miR-200 family promotes EMT and invasion in cancer cells. EMBO Rep 2008; 9: 582-9.
[55] Smith CM, Watson DI, Leong MP, Mayne GC, Michael MZ, Wijnhoven BP, Hussey DJ. miR-200 family expression is downregulated upon neoplastic progression of Barrett's esophagus. World J Gastroenterol 2011; 17: 1036.
[56] Hur K, Toiyama Y, Takahashi M, Balaguer F, Nagasaka T, Koike J, Hemmi H, Koi M, Boland CR, Goel A. MicroRNA-200c modulates epithelial-to-mesenchymal transition (EMT) in human colorectal cancer metastasis. Gut 2013; 62: 1315-26.
[57] Yu J, Ohuchida K, Mizumoto K, Sato N, Kayashima T, Fujita H, Nakata K, Tanaka M. MicroRNA, hsa-miR-200c, is an independent prognostic factor in pancreatic cancer and its upregulation inhibits pancreatic cancer invasion but increases cell proliferation. Mol Cancer 2010; 9: 169.
[58] Lee H, Jun SY, Lee YS, Lee HJ, Lee WS, Park CS. Expression of miRNAs and ZEB1 and ZEB2 correlates with histopathological grade in papillary urothelial tumors of the urinary bladder. Virchows Arch 2014; 464: 213-20.
[59] Wszolek MF, Rieger-Christ KM, Kenney PA, Gould JJ, Silva Neto B, Lavoie AK, Logvinenko T, Libertino JA, Summerhayes IC. A MicroRNA expression profile defining the invasive bladder tumor phenotype. Urol Oncol 2011; 29: 794-801, e1.